Int. J. Heat Mass Transfer. Vol. 31, No. 9, pp. 1759–1766, 1988
Printed in Great Britain

0017–9310/88 $3.00 + 0.00
Pergamon Press plc

Transient natural convection in triangular enclosures

YU. E. KARYAKIN and YU. A. SOKOVISHIN
Kalinin Polytechnical Institute, 195251, Leningrad, U.S.S.R.

and

O. G. MARTYNENKO
Luikov Heat and Mass Transfer Institute, 220728, Minsk, U.S.S.R.

(*Received* 15 *July* 1985)

Abstract—The analysis is carried out for laminar natural convection in a prismatic enclosure the cross-section of which constitutes an isosceles triangle. Two cases of thermal boundary conditions are considered: (a) the horizontal base is adiabatic, while the inclined walls are isothermal (cold and hot); (b) all the solid surfaces are isothermal (hot inclined surfaces and cold bottom). The finite-difference method for solving the non-stationary Navier–Stokes and energy equations is described which utilizes the physical variables velocity–pressure–temperature. The numerical solution of the problem is presented for Grashof numbers $10^3 \leqslant Gr \leqslant 10^8$ and height-to-base ratios $0.25 \leqslant H/L \leqslant 2$. It has been found that the maximum values of the stream function and Nusselt numbers may perform damping oscillations around their steady-state values. At high Gr, gradient regions of the type of dynamic and thermal boundary layers are formed on all the solid surfaces and the temperature distribution in the central part of the enclosure approaches the conditions of fluid stratification. The present results are in good agreement with experimental data of other authors.

1. INTRODUCTION

THERE have recently been considerable advances in the study of the phenomena of natural convection in enclosures of an arbitrary configuration thanks to successes in the development of efficient methods for solving Navier–Stokes equations and the advent of large-capacity electronic computers, i.e. to the possibility of carrying out the so-called numerical experiment on a large scale.

A great number of works, in which numerical methods were used, are concerned with the investigation of convection in rectangular cavities [1–3]. Being of practical importance, this problem is a test one for checking and comparing different numerical methods. Of interest in this respect are refs. [4, 5], where dozens of numerical methods have been verified in detail on the example of natural convection in a square enclosure with lateral heating.

Actual enclosures occurring in practice often have the shape differing from the rectangular. Thus, various channels of constructions, panels of electronic equipment, current leads in the electrotechnical industry, and solar energy collectors are of the form of triangular prisms.

The first numerical simulation of convection in an enclosure of triangular cross-section can be found in ref. [6]. Specific features of two types of fluid motion are investigated in the cavity with bottom heating at over-critical Rayleigh numbers. In ref. [7], a prismatic enclosure of the right triangle cross-section is considered in which the horizontal base is cooled and the vertical wall is adiabatic. Convection arises from the heating of the inclined wall. Stationary solutions of the problem are found within the ranges $0.0625 \leqslant H/L \leqslant 1$ and $800 \leqslant Gr \leqslant 6.4 \times 10^4$. Further results were given by the same authors elsewhere [8]. An analogous problem was solved [9] by the method of finite elements.

The unsteady-state natural convection in an enclosure with the cross-section in the form of an isosceles triangle was studied in ref. [10]. All the walls of the enclosure were assumed to be isothermal, the base to be heated and the side surfaces to be cooled. The problem was solved by three techniques: asymptotic expansion of unknown quantities in the small geometric parameter H/L, an analysis of the change in the scales of dependent variables in the process of convection development, and finally, calculation with the aid of the finite-difference method. When $H/L \to 0$, the total heat flux is shown to be governed by heat conduction. At finite values of H/L, dynamic and thermal wall layers develop on the surfaces of the enclosure. In the process of transition, velocity and stream function profiles attain their steady-state values in an oscillatory manner rather than monotonically.

Experimental study of heat transfer by natural convection in triangular enclosures with different temperature conditions on the walls was made in refs. [11–13].

In ref. [11], an enclosure with the cross-section of

NOMENCLATURE

c_p	heat capacity at constant pressure
D	function defined by equation (13)
F_1, F_2	functions defined by equations (9) and (10)
g	gravitational acceleration
Gr	Grashof number, $\beta g(T_h - T_c)L^3/\nu^2$
H	height of enclosure
l	relative coordinate reckoned along the inclined wall from the enclosure base; $l = 1$ corresponds to the enclosure apex
L	width of enclosure base
n	coordinate orthogonal to the inclined wall
Nu	local Nusselt number, $(\partial\theta/\partial n)_w$
Nu'	relative local Nusselt number
p	dimensionless pressure
$\hat{p}$	function defined by equation (11)
Pr	Prandtl number, $\rho\nu c_p/\lambda$
S	source term in equation (13)
t	dimensionless time
T	temperature
u	dimensionless horizontal velocity component
v	dimensionless vertical velocity component
x	dimensionless horizontal coordinate
y	dimensionless vertical coordinate.

Greek symbols

α	weighted coefficient
β	coefficient of volumetric thermal expansion
Δ	increment of the value
θ	relative temperature, $(T - T_c)/(T_h - T_c)$
$\kappa_R, \kappa_L, \kappa_U, \kappa_D$	coefficients determined by boundary conditions
λ	thermal conductivity
$\Lambda, \Lambda_1, \Lambda_2$	finite-difference operators
ν	kinematic viscosity of fluid
ξ	pressure correction
ρ	density of fluid
τ	relaxation time
ψ	stream function.

Subscripts

c	on the cold wall
h	on the hot wall
i, j	grid indices in the direction of the x- and y-axes, respectively
m	number of steps $\Delta\tau$
w	solid surface
0	scale of the quantity.

Superscripts

n	number of the time layer
s	number of iteration.

an isosceles triangle was considered the base of which was insulated and the inclined walls were isothermal (hot and cold). The range of Grashof numbers $3.9 \times 10^6 \leqslant Gr \leqslant 9.03 \times 10^6$ was studied for three apex angles: 60°, 90° and 120°. It is shown that there are high temperature gradients near the surfaces, with liquid stratification occurring in the central part of the enclosure.

Heat transfer in triangular enclosures heated or cooled from below was studied in ref. [12]. With cooling from below the flow remained stable and laminar within the range of Grashof numbers $1.75 \times 10^5 \leqslant Gr \leqslant 5.08 \times 10^6$. When the bottom of the enclosure was heated, then at some Grashof numbers the flow acquired a turbulent character.

The range of high Rayleigh numbers (from 10^6 to 10^9), typical for full-scale attics or littoral zones of seas and oceans with sloping bottoms, was studied in ref. [13]. The region of convection has the cross-section in the form of a right triangle the hypotenuse of which is cooled, the horizontal side is heated and the vertical side is insulated. A sinusoidal flow structure at the enclosure base is revealed.

The overwhelming majority of works on numerical simulation of natural convection is based on the use of the variables 'stream function–vorticity–temperature'. Numerical methods based on the use of the physical variables 'velocity–pressure–temperature' have been in development only from the late 1960s. The chief merits of these methods are: simple and natural formulation of boundary conditions, possibility to be directly extended to three-dimensional cases of motion. The physical variables were successfully used in ref. [14] for solving the Navier–Stokes equations by the method of markers and cells. In refs. [15, 16], weak artificial compressibility is introduced for studying the motion of a non-compressible fluid. Effective methods of solving the problems of heat transfer and fluid dynamics are given in refs. [17, 18].

This paper considers the use of the finite-difference method, based on the physical variables, for calculation of transient natural convection in a triangular enclosure. Some aspects of the solution of this problem are given elsewhere [19–21].

2. MATHEMATICAL FORMULATION

Consider rather a long prismatic enclosure with the cross-section in the form of an isosceles triangle (Fig. 1). The gravity vector is normal to the base.

The assumptions about the character of fluid convection in the enclosure are as follows:

(a) the flow is two-dimensional and laminar;

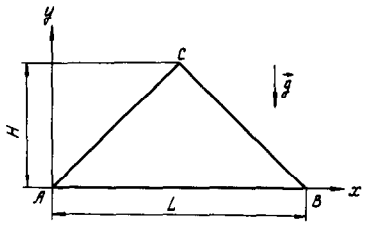

FIG. 1. Triangular convection region.

(b) there are moderate temperature gradients for which the Boussinesq approximation is valid;

(c) viscous dissipation and the work done by compression forces are negligible.

With the use of these assumptions the basic equations for the unsteady-state natural convection can be written in the dimensionless form [21] as

$$\frac{\partial u}{\partial x}+\frac{\partial v}{\partial y}=0 \tag{1}$$

$$\frac{\partial u}{\partial t}+\frac{\partial (u^2)}{\partial x}+\frac{\partial (uv)}{\partial y}=-\frac{\partial p}{\partial x}+\frac{\partial^2 u}{\partial x^2}+\frac{\partial^2 u}{\partial y^2} \tag{2}$$

$$\frac{\partial v}{\partial t}+\frac{\partial (uv)}{\partial x}+\frac{\partial (v^2)}{\partial y}=Gr\,\theta-\frac{\partial p}{\partial y}+\frac{\partial^2 v}{\partial x^2}+\frac{\partial^2 v}{\partial y^2} \tag{3}$$

$$\frac{\partial \theta}{\partial t}+\frac{\partial (u\theta)}{\partial x}+\frac{\partial (v\theta)}{\partial y}=\frac{1}{Pr}\left(\frac{\partial^2 \theta}{\partial x^2}+\frac{\partial^2 \theta}{\partial y^2}\right). \tag{4}$$

For the construction of dimensionless quantities the linear scale is selected to be the width of the enclosure base L, the time scale the diffusion time $t_0=L^2/\nu$, the velocity scale the quantity $u_0=L/t_0=\nu/L$, and the pressure scale is taken to be twice the dynamic pressure $\rho u_0^2=\rho\nu^2/L^2$.

Equations (1)–(4) are augmented with corresponding boundary and initial conditions. The usual non-slip and non-flow conditions are adopted for the velocity vector components on impermeable solid surfaces. The temperature boundary conditions are specified in two ways. In the first case the inclined walls are assumed to be isothermal (hot and cold) and the base to be insulated. In the second case all the enclosure surfaces are taken to be isothermal: the inclined walls to be hot and the base to be cold. With allowance for the above, the boundary conditions can be written as

Case I

$$\begin{aligned}
&u=v=0,\ \theta=1 \quad \text{for } 0\leqslant x\leqslant 0.5,\ y=2Hx/L\\
&u=v=0,\ \theta=0 \quad \text{for } 0.5<x\leqslant 1,\ y=2H(1-x)/L\\
&u=v=0,\ \partial\theta/\partial y=0 \quad \text{for } 0\leqslant x\leqslant 1,\ y=0
\end{aligned} \tag{5}$$

Case II

$$\begin{aligned}
&u=v=0,\ \theta=1 \quad \text{for } 0\leqslant x\leqslant 0.5,\ y=2Hx/L\\
&u=v=0,\ \theta=1 \quad \text{for } 0.5\leqslant x\leqslant 1,\ y=2H(1-x)/L\\
&u=v=0,\ \theta=0 \quad \text{for } 0<x<1,\ y=0.
\end{aligned} \tag{6}$$

When solving the problem in physical variables, the pressure p is determined from equations (2) and (3) accurate to an arbitrary constant. For the sake of definiteness, it will be assumed that $p=0$ at the point with the coordinates $x=y=0$.

The assumed initial conditions are that the fluid is motionless and the temperature field is uniform throughout the entire convection region, i.e.

$$t=0,\quad u=v=0,\quad \theta=0.5.$$

3. METHOD OF SOLUTION

Integrate equations (2) and (3) over the time from t to $t+\Delta t$

$$u(t+\Delta t)=F_1(t)-\frac{\partial \hat{p}}{\partial x}\Delta t \tag{7}$$

$$v(t+\Delta t)=F_2(t)-\frac{\partial \hat{p}}{\partial y}\Delta t \tag{8}$$

where

$$F_1(t)=u(t)+\left[\frac{\partial^2 u}{\partial x^2}+\frac{\partial^2 u}{\partial y^2}-\frac{\partial (u^2)}{\partial x}-\frac{\partial (uv)}{\partial y}\right]\Delta t \tag{9}$$

$$F_2(t)=v(t)+\left[\frac{\partial^2 v}{\partial x^2}+\frac{\partial^2 v}{\partial y^2}-\frac{\partial (uv)}{\partial x}-\frac{\partial (v^2)}{\partial y}+Gr\,\theta\right]\Delta t \tag{10}$$

$$\hat{p}=\frac{1}{\Delta t}\int_t^{t+\Delta t} p\,\mathrm{d}t. \tag{11}$$

Functions $u(t+\Delta t)$ and $v(t+\Delta t)$, which are determined from equations (7) and (8) with the use of function $\hat{p}$, should satisfy the condition of solenoidality, i.e. continuity equation (1). Henceforth the symbol ($\hat{}$) over function p will be omitted.

The unknown function p can be found from the following evolutional equation which is constructed on the basis of continuity equation (1) with the addition of the term $\partial p/\partial\tau$ [21]

$$\frac{\partial p}{\partial \tau}+D(p)=0 \tag{12}$$

where $D(p)$, with equations (7) and (8) taken into account, has the form

$$D(p)\equiv\frac{\partial u}{\partial x}+\frac{\partial v}{\partial y}=-\left(\frac{\partial^2 p}{\partial x^2}+\frac{\partial^2 p}{\partial y^2}\right)\Delta t+S \tag{13}$$

and the source term $S=\partial F_1/\partial x+\partial F_2/\partial y$.

To construct the difference scheme, the convection region is marked with rectangular grids of the unknown values u, v, θ and p which are displaced relative to one another as is conventional in the method of markers and cells [14]. The nodes of the grids will be fitted to the boundaries of the triangular

convection region, then the steps Δx and Δy will be connected by the relation $\Delta y = 2H\Delta x/L$. The difference analogue of expressions (7) and (8) on the shifted grids will be presented in the form

$$u^{n+1}_{i+1/2,j} = F^n_{1i+1/2,j} - \frac{\Delta t}{\Delta x}(p_{i+1,j} - p_{i,j}) \quad (14)$$

$$v^{n+1}_{i,j+1/2} = F^n_{2i,j+1/2} - \frac{\Delta t}{\Delta y}(p_{i,j+1} - p_{i,j}). \quad (15)$$

Let the finite-difference operators Λ_1 and Λ_2 approximate the partial differential operators $\partial^2/\partial x^2$ and $\partial^2/\partial y^2$, respectively, with the second order of approximation. To solve equation (12), use will be made of the iterative finite-difference scheme with spatial splitting

$$\frac{\xi^{s+1/2}}{\Delta\tau} - \alpha\Delta t\Lambda_1(\xi^{2+1/2}) + D(p^s) = 0 \quad (16)$$

$$\frac{\xi^{s+1} - \xi^{s+1/2}}{\Delta\tau} - \alpha\Delta t\Lambda_2(\xi^{s+1}) = 0 \quad (17)$$

$$p^{s+1} = p^s + \xi^{s+1}. \quad (18)$$

By ruling out the fractional step from equations (16) and (17), it is possible to obtain an equivalent scheme ($\Lambda = \Lambda_1 + \Lambda_2$)

$$\frac{p^{s+1} - p^s}{\Delta\tau} = \Lambda t\Lambda[\alpha p^{s+1} + (1-\alpha)p^s]$$

$$-S - (\alpha\Delta t\Delta\tau)^2\Lambda_1\left[\Lambda_2\left(\frac{p^{s+1} - p^s}{\Delta\tau}\right)\right]. \quad (19)$$

At $\alpha = 0.5$, scheme (19) approximates the initial equation (12) with the approximation of $O(\Delta\tau^2)$.

It is convenient to present the finite-difference equations (16) and (17) for the pressure corrections in the form which takes into account the boundary conditions for velocity components

$$\frac{\xi^{s+1/2}_{i,j}}{\Delta\tau} - \frac{\alpha\Delta t}{\Delta x^2}[\kappa_R(\xi^{s+1/2}_{i+1,j} - \xi^{s+1/2}_{i,j}) - \kappa_L(\xi^{s+1/2}_{i,j} - \xi^{s+1/2}_{i-1,j})] + D^s_{i,j} = 0 \quad (20)$$

$$\frac{\xi^{s+1}_{i,j} - \xi^{s+1/2}_{i,j}}{\Delta\tau} - \frac{\alpha\Delta t}{\Delta y^2}[\kappa_U(\xi^{s+1}_{i,j+1} - \xi^{s+1}_{i,j}) - \kappa_D(\xi^{s+1}_{i,j} - \xi^{s+1}_{i,j-1})] = 0. \quad (21)$$

When any boundary of the MAC cell coincides with the boundary of the convection region, then the corresponding coefficient from the succession κ_R, κ_L, κ_U and κ_D vanishes. Otherwise it will be equal to 1. The coefficient κ_R is responsible for the right boundary of the MAC cell, κ_L for the left, κ_U for the upper and κ_D for the lower boundary. Thus, boundary conditions (5) and (6) for velocity components u and v are satisfied automatically. There are no other special boundary conditions for function p.

Equations (20) and (21) are solved by successive scalar sweeping processes along the x- and y-directions [22]. Near the corner points of the enclosure, the finite-difference equations (20) and (21) are degenerate as is peculiar to the sweeping method in the regions of triangular shape. To accelerate the iterative process, the following sequence of steps $\Delta\tau\{\Delta\tau_0, \Delta\tau_1, \ldots, \Delta\tau_m\}$ is used, which ensures a uniform convergence of the solution over the entire spectrum of eigenvalues of the problem.

When the above finite-difference method is applied, the sequence of operations is as follows:

(1) using the known values of the functions u^n, v^n and θ^n, functions F^n_1 and F^n_2 are calculated on the nth time layer with the aid of expressions (9) and (10);

(2) the field of function p is determined by iterations from equations (20), (21) and (18);

(3) functions u^{n+1} and v^{n+1} are determined on a new, $(n+1)$th, time layer with the aid of expressions (14) and (15);

(4) the field of the relative temperature θ^{n+1} is determined from the finite-difference analogue of equation (4);

(5) the transition to the next time layer is carried out.

Calculations were carried out on a difference grid with 40 nodes along the vertical line and 80 nodes along the enclosure base. The time for calculating one version of the unsteady-state problem ($Gr = 10^4$) on an electronic computer BESM-6 amounts to about 30 min.

4. NUMERICAL RESULTS AND DISCUSSION

4.1. *Case* I (*insulated base*)

In this case the thermal boundary conditions have the form of equations (5). They demand that the base AB of the triangular enclosure (Fig. 1) is insulated and the inclined surfaces are isothermal (AC is hot, BC is cold).

First, the problem was solved which had been studied experimentally in ref. [11]. The parameters of the experiment are as follows: $T_h = 322$ K, $T_c = 274$ K, $L = 0.1524$ m, $H/L = 0.5$, $Pr = 0.71$, $Gr = 2.1577 \times 10^7$. Figure 2 presents the distribution of the local Nusselt number $Nu(l) = \partial\theta/\partial n|_w$ along the surface of the cold side wall BC under the steady-state convection conditions, $l = 0$ at point B, $l = 1$ at point C. The solid line presents the results of the numerical solution of the problem by the above-described method.

The coincidence between the numerical and experimental results should be accepted as satisfactory, the more so that the requirement for base insulation was not strictly met in the experiment, neither strictly observed were the conditions of isothermicity on the side surfaces near apex C of the enclosure. In a certain sense, this point is a singular one for the initial convection equations, since it is at this point that the isothermal surfaces with $\theta = 0$ and 1 intersect. Accordingly, the local Nusselt number should become infinite at point C.

Systematic calculations of the natural convection

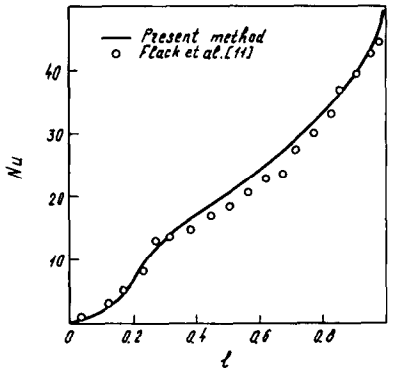

FIG. 2. Distribution of the local Nusselt number along cold wall BC. Comparison with experiment.

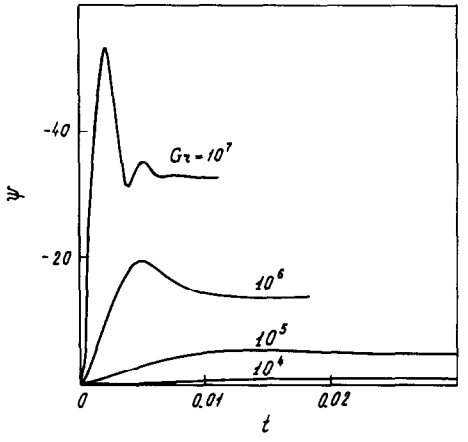

FIG. 3(a). The influence of Gr on function $\psi(t)$ at the enclosure point with the coordinates $x = 0.5$ and $y = 0.5H/L$.

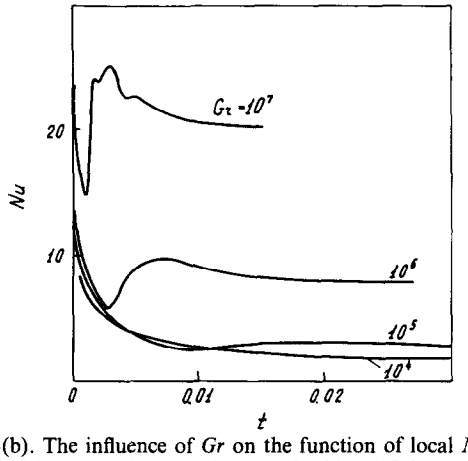

FIG. 3(b). The influence of Gr on the function of local Nu with time at the central point of cold wall BC.

were made in the range of Grashof numbers $10^3 \leqslant Gr \leqslant 10^8$ and of the values of the geometrical parameter H/L: $0.25 \leqslant H/L \leqslant 2$. It was assumed that $Pr = 1$.

Figure 3(a) shows the time history of the stream function at the fixed enclosure point with the coordinates $x = 0.5$ and $y = 0.5H/L$ at $H = 0.5L$ for four values of Gr: 10^4, 10^5, 10^6, and 10^7. The values of the local Nusselt number at the central point of the cold wall are given in Fig. 3(b) for the same parameters.

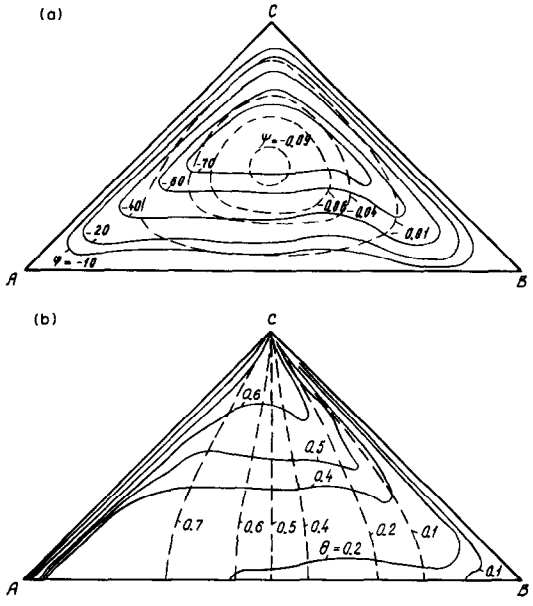

FIG. 4. Stream lines (a) and isotherms (b) in the steady-state convection regime at $H/L = 0.5$. The dashed lines correspond to $Gr = 10^3$, solid lines correspond to $Gr = 10^8$.

At comparatively small Grashof numbers, $Gr \leqslant 10^4$, the values of the stream function ψ, which characterize the intensity of convective motion in the enclosure, increase monotonously with time approaching a certain limit. A circulation zone is formed in the flow region with fluid circulating in a clockwise direction.

When $Gr \geqslant 10^5$, the functions $\psi(t)$ and $Nu(t)$ are no longer of monotonous character. At $Gr = 10^5, 10^6$, the stream function exhibits a maximum, and thereafter decreases to some limiting value. When $Gr \geqslant 10^7$, the quantity ψ, on having reached the maximum, tends to a stationary value according to the law of damping oscillations. In these cases the function $Nu(t)$ is also non-monotonous. As follows from Fig. 3, the time for the development of the unsteady-state process decreases with an increasing Grashof number.

The influence of the Grashof number on the location of stream lines is demonstrated in Fig. 4(a). Corresponding isotherms are given in Fig. 4(b).

When $Gr \sim 10^3$, the processes occurring in the enclosure are mainly determined by heat conduction. In the central part of the enclosure the isotherms take on almost a vertical position (Fig. 4(b), dashed lines).

With the growth of the Grashof number the intensity of convective processes increases, at $Gr = 10^8$ they fully predominate over heat conduction. On the solid surfaces there appear regions which resemble dynamic boundary layers, and gradient zones of the type of thermal boundary layers are formed on the side walls. In the central part of the enclosure the isotherms take horizontal positions, which corresponds to the conditions of fluid stratification (Fig. 4(b), solid lines).

An investigation was made of the influence of the geometrical parameter H/L on the main charac-

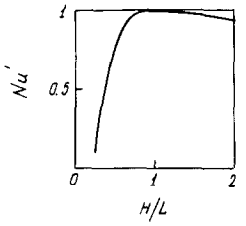

FIG. 5. The dependence of relative Nu' at the central point of cold wall BC on geometrical parameter H/L.

teristics of convection in a triangular enclosure. In Fig. 5 the dependence of the relative value, Nu', of the local Nusselt number at the central point of the cold wall BC on the geometrical parameter H/L is given for $Gr = 10^6$. The scale for the construction of Nu' is selected to be the maximum value of Nu.

It follows from Fig. 5 that at a fixed Grashof number the intensity of convective processes in an enclosure first sharply increases with the growth of the parameter H/L. At $H/L \approx 1$ the maximum of Nu is observed at the central point of the cold wall, then its value slightly decreases with an increase of H/L.

4.2. *Case* II (*isothermal walls*)

In this case the boundary conditions have the form of equations (6) and demand that all the surfaces of the enclosure are isothermal, the base AB is cold and the inclined walls AB and BC are hot. These are the conditions, for instance, in which solar energy collectors and attic constructions are exposed to during the daytime.

Such a problem was investigated experimentally in ref. [12]. One of the convection regimes in the experiment is characterized by the following parameters: $T_h = 323$ K, $T_c = 273$ K, $L = 0.1524$ m, $H = 0.5L$, $Pr = 0.71$. The corresponding Grashof number of the regime is $Gr = 2.272 \times 10^7$.

In Fig. 6 the comparison is given between the results calculated by the above-described method and the data from ref. [12]. The distribution of the local Nusselt number $Nu(l)$ along the surface of the inclined wall AC is given as well as the distribution of the dimensionless temperature θ on the vertical symmetry axis $x = 0.5$ of the triangular enclosure in the steady-state regime. The solid lines present the results of the numerical solution. The agreement of the results should be good.

There is some discrepancy for Nu near point A of the enclosure ($l \approx 0$). In the case of rigorous formulation of the thermal boundary conditions on walls AB and AC ($\theta_c = 0$, $\theta_h = 1$) point A becomes a singular one. The local Nusselt number must turn into infinity at this point, and the integral of Nu along the inclined surface simply does not exist [21]. The data presented in ref. [12] indicate that, generally speaking, the conditions of the isothermicity of the walls near the corner points were violated in the experiment. The height-to-base ratio varied in calculations within the range $0.25 \leqslant H/L \leqslant 2$, the Grashof number changed

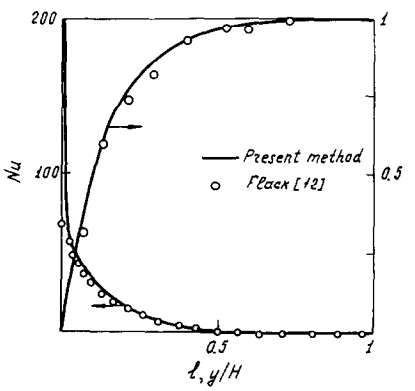

FIG. 6. Variation of local Nu along the surface of the inclined wall AC and distribution of temperature θ along the symmetry line of a triangular enclosure. Comparison with experiment.

within the range $10^3 \leqslant Gr \leqslant 10^7$, it was assumed that $Pr = 1$. The original convection equations with boundary conditions (6) presuppose the existence of the solution symmetry about the vertical axis which passes through the enclosure apex C

$$u(x, y) = -u(1-x, y)$$
$$v(x, y) = v(1-x, y)$$
$$p(x, y) = p(1-x, y)$$
$$\theta(x, y) = \theta(1-x, y).$$

Nevertheless, the symmetry conditions were not used when the difference algorithm was applied. To control the accuracy of numerical results, the problem was solved for the entire convection region.

Figure 7 shows the variation in time of the maximum values of the stream function ψ in the triangular enclosure at $H = 0.5L$ and four Grashof numbers: 10^4, 10^5, 10^6, and 10^7. When $Gr \leqslant 10^4$, the stream function tends practically monotonously to its steady-state value. In the left half of the enclosure the fluid circulates in a clockwise sense. When $Gr \geqslant 10^5$, the function $\psi_{max}(t)$ ceases to be monotonous. At a certain instant the quantity ψ_{max} attains a maximum and then, decreases to a steady-state value. It is characteristic of this type of boundary conditions (6) that the function $\psi_{max}(t)$ does not exhibit an oscillatory character. Thus, the triangular enclosure with isothermal surfaces possesses increased damping properties.

The influence of Grashof number on the position of stream lines and isotherms at $H/L = 0.5$ is presented in Fig. 8. With the growth of Gr the centres of circulation zones shift to the corner points of the triangular base, the intensity of convection in the upper part of the enclosure decreases and the temperature distribution approaches the conditions of fluid stratification.

The analysis of numerical results has shown that in the upper part of the enclosure the heat fluxes on the wall are small; they decrease with an increase of the Grashof number and with the growth of the geo-

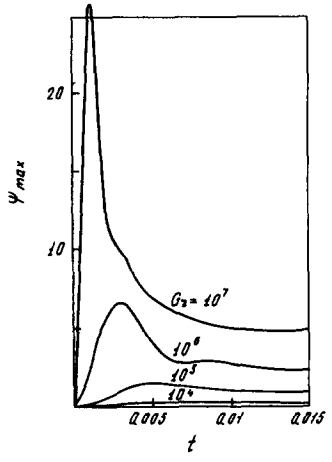

FIG. 7. The dependence $\psi_{max}(t)$ in a triangular enclosure with isothermal walls.

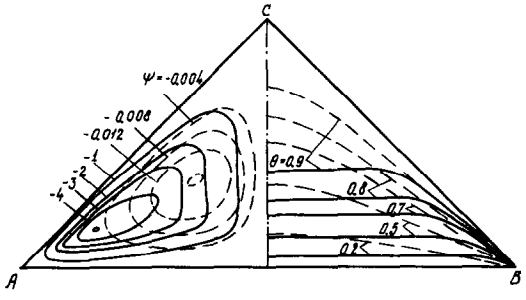

FIG. 8. Stream lines (left) and isotherms (right) in the steady-state convection regime. Dashed lines correspond to $Gr = 10^3$, solid lines correspond to $Gr = 10^7$.

metrical parameter H/L. At high values of Gr and H/L the fluid temperature on the symmetry axis for $y \geqslant 0.5H/L$ is virtually equal to the temperature of the side walls, i.e. in the upper part of the enclosure the fluid has a homogeneous temperature. In this region the buoyancy forces are small, as well as heat fluxes through the inclined walls.

As a result of the analysis of numerical data on the convection in a triangular enclosure with isothermal walls the formula is obtained which correlates the local Nusselt number on the surface of the heated wall AC with Gr, H/L and with the relative coordinate l of a point on the wall

$$Nu = 0.083\frac{1-l}{l}\left(\frac{H}{L}\right)^{-1} Gr^{0.13} \cdot 10^{f} \qquad (22)$$

where

$$f = 1 - 12 \cdot 2.6^{-\sqrt{(H/L)\log Gr}} + (3.21 - 0.87\sqrt{(H/L)\log Gr})l.$$

Equation (22) reveals an essential influence of H/L on the Nu distribution along the inclined surface. This formula approximates rather well the numerical data in the region of Grashof numbers $10^3 \leqslant Gr \leqslant 10^7$ and geometric parameters $0.25 \leqslant H/L \leqslant 2$ for $l > 0.15$.

5. CONCLUSIONS

(1) The finite-difference method is developed for solving the non-stationary Navier–Stokes and energy equations in the variables velocity–pressure–temperature. Using this method the natural convection in a region bounded by an isosceles triangle is studied.

(2) The regions of the values of the Grashof number $10^3 \leqslant Gr \leqslant 10^8$ and of the geometrical parameter $0.25 \leqslant H/L \leqslant 2$ are investigated. Two cases of thermal boundary conditions are examined: lateral heating of the enclosure with an insulated base and heating from above. The results of calculations agree with the available experimental data.

(3) At high values of Gr steady state is achieved non-monotonically. In some cases the maximum values of the stream function in an enclosure accomplish damping oscillations around their steady-state values. The heating of the enclosure from above exerts a higher damping influence on the process of convection development than in the case of lateral heating.

(4) In the case of the lateral heating of an enclosure and high Gr, gradient regions, which resemble dynamic and thermal boundary layers, are formed on inclined walls. With the growth of Gr the isotherms in the central part of the enclosure take the horizontal position, which corresponds to the conditions of fluid stratification.

REFERENCES

1. G. Z. Gershuni, E. M. Zhukhovitskiy and E. L. Tarunin, Numerical investigation of natural convection in a closed cavity, *Izv. AN SSSR, Mekh. Zhidk. Gaza* No. 5, 56–62 (1966).
2. I. P. Jones, A numerical study of natural convection in an air-filled cavity: comparison with experiment, AERE-R9346, Harwell (1978).
3. T. N. Phillips, Natural convection in an enclosed cavity, *J. Comput. Phys.* **54**, 365–381 (1984).
4. G. de V. Davis and I. P. Jones, Natural convection in a square cavity—a comparison exercise. In *Numerical Methods in Thermal Problems*, pp. 552–572. Swansea (1981).
5. I. P. Jones and C. P. Thompson (Editors), Numerical solution for a comparison problem on natural convection in an enclosed cavity, AERE-R9955, Harwell (1981).
6. G. Z. Gershuni, E. M. Zhukhovitskiy and D. L. Shvartzblat, Overcritical convective motions in asymmetric region. In *Hydrodynamics*, No. 7, pp. 89–95. Perm (1974).
7. V. A. Akinsete and T. A. Coleman, Heat transfer by steady laminar free convection within triangular enclosures. In *Numerical Methods in Thermal Problems*, pp. 259–268. Swansea (1979).
8. V. A. Akinsete and T. A. Coleman, Heat transfer by steady laminar free convection in triangular enclosures, *Int. J. Heat Mass Transfer* **25**, 991–998 (1982).
9. H. S. Kushwaha, Finite element computation of natural convection in enclosures, Bhabha Atomic Research Centre, BARC-1148 (1982).
10. D. Poulikakos and A. Bejan, The fluid dynamics of an attic space, *J. Fluid Mech.* **131**, 251–269 (1983).
11. R. D. Flack, T. T. Konopnicki and J. H. Rooke, The measurement of natural convective heat transfer in tri-

angular enclosures, *Trans. Am. Soc. Mech. Engrs*, Series C, *J. Heat Transfer* **101**, 648–654 (1979).
12. R. D. Flack, The experimental measurements of natural convection heat transfer in triangular enclosures heated or cooled from below, *Trans. Am. Soc. Mech. Engrs*, Series C, *J. Heat Transfer* **102**, 770–772 (1980).
13. D. Poulikakos and A. Bejan, Natural convection experiments in a triangular enclosure, *Trans. Am. Soc. Mech. Engrs*, Series C, *J. Heat Transfer* **105**, 652–655 (1983).
14. F. H. Harlow and J. E. Welch, Numerical calculation of time-dependent viscous incompressible flow of fluid with free surface, *Physics Fluids* **8**, 2182–2189 (1965).
15. N. N. Vladimirova, V. G. Kuznetsov and N. N. Yanenko, Numerical calculation of symmetric two-dimensional viscous incompressible fluid flow past a flat plate. In *Some Problems of Applied and Computational Mathematics*, pp. 186–192. Novosibirsk (1966).
16. A. J. Chorin, Numerical solution of the Navier–Stokes equations, *Math. Comput.* **22**, 745–762 (1968).
17. S. Patankar, *Numerical Heat Transfer and Fluid Flow*. Hemisphere, New York (1980).
18. O. M. Belotserkovskiy, *Numerical Simulation in Continuum Mechanics*. Izd. Nauka, Moscow (1984).
19. Yu. E. Karyakin and Yu. A. Sokovishin, Unsteady-state natural convection in a triangular enclosure with isothermal walls, *Izv. AN SSSR, Ser. Fiz. Energ. Nauk* No. 4, 104–110 (1985).
20. Yu. E. Karyakin and Yu. A. Sokovishin, Unsteady-state natural convection in an enclosure of triangular cross-section, *Izv. AN SSSR, Mekh. Zhidk., Gaza* No. 5, 169–173 (1985).
21. Yu. E. Karyakin, O. G. Martynenko, Yu. A. Sokovishin and Kh. Z. Ustok, Numerical simulation of unsteady-state natural convection in triangular enclosures, *Heat Transfer—Sov. Res.* **17**(3), 1–33 (1985).
22. R. Peyret and J. D. Taylor, *Computational Methods for Fluid Flow*. Springer, New York (1983).

CONVECTION NATURELLE VARIABLE DANS DES ENCEINTES TRIANGULAIRES

Résumé—On étudie la convection naturelle laminaire dans une enceinte prismatique dont la section droite est un triangle isocèle. On considère deux cas de conditions aux limites: (a) la base horizontale est adiabatique, tandis que les parois inclinées sont isothermes (chaudes et froides); (b) toutes les surfaces sont isothermes (surfaces inclinées chaudes et base froide). La méthode des différences finies utilisée pour résoudre les équations de Navier–Stokes et d'énergie en régime variable utilise les variables physiques vitesse–pression–température. La solution numérique est donnée pour le nombre de Grashof $10^3 \leqslant Gr \leqslant 10^8$ et le rapport hauteur sur base $0{,}25 \leqslant H/L \leqslant 2$. On trouve que les valeurs maximales de la fonction de courant et du nombre de Nusselt peuvent subir des oscillations amorties autour des valeurs de régime permanent. Pour Gr élevé, des régions de gradient du type des couches limites dynamique et thermique se trouvent sur toutes les surfaces solides et la distribution de température dans la paroi centrale de l'enceinte s'approche des conditions de stratification du fluide. Les résultats sont en bon accord avec les données expérimentales d'autres auteurs.

TRANSIENTE NATÜRLICHE KONVEKTION IN HOHLRÄUMEN VON DREIECKIGEM QUERSCHNITT

Zusammenfassung—Die laminare natürliche Konvektion in einem prismatischen Hohlraum von gleichschenklig-dreieckigem Querschnitt wird analytisch untersucht. Zwei unterschiedliche Randbedingungen werden betrachtet: (a) die waagerechte Grundfläche ist adiabat, während die beiden geneigten Wandflächen isotherm (heiß bzw. kalt) sind; (b) sämtliche Wandflächen sind isotherm (die geneigten heiß und die untenliegende kalt). Die nicht-stationären Navier–Stokes- und Energiegleichungen werden unter Verwendung der physikalischen Variablen Geschwindigkeit-Druck-Temperatur mit Hilfe eines Finite-Differenzen-Verfahrens gelöst. Numerische Ergebnisse werden für Grashof-Zahlen $10^3 \leqslant Gr \leqslant 10^8$ und Höhe/Grundkanten-Verhältnisse $0{,}25 \leqslant H/L \leqslant 2$ vorgestellt. Es zeigt sich, daß die Maximalwerte von Stromfunktion und Nusselt-Zahl gedämpfte Schwingungen um den jeweiligen stationären Wert ausführen. Bei hoher Gr-Zahl bilden sich an allen festen Oberflächen Gradientengebiete vom Typ dynamischer und thermischer Grenzschichten aus. Die Temperaturverteilung im Kerngebiet des Hohlraumes nähert sich einem geschichteten Zustand.

НЕСТАЦИОНАРНАЯ ЕСТЕСТВЕННАЯ КОНВЕКЦИЯ В ТРЕУГОЛЬНЫХ ЕМКОСТЯХ

Аннотация—Исследуется ламинарная естественная конвекция в призматической емкости, поперечное сечение которой—равнобедренный треугольник. Рассматриваются два случая температурных граничных условий: (а) горизонтальное основание теплоизолировано, наклонные стенки изотермические (холодная и горячая); (в) все твёрдые поверхности изотермические (наклонные—горячие, основание—холодное). Описывается конечно-разностный метод решения нестационарных уравнений Навье–Стокса и энергии, использующий физические переменные скорость–давление–температура. Решение задачи получено в диапазоне чисел Грасгофа $10^3 \leqslant Gr \leqslant 10^8$ и отношений высоты емкости к основанию $0.25 \leqslant H/L \leqslant 2$. Установлено, что максимальные значения функции тока и значения числа Нуссельта могут совершать затухающие колебания вблизи их стационарных величин. При больших значениях числа Gr на твёрдых поверхностях образуются градиентные зоны типа динамических и температурных пограничных слоёв, а распределение температуры в центральной части емкости приближается к условиям стратификации жидкости. Полученные результаты согласуются с экспериментальными данными других авторов.